# Estimation of low-latitude irregularity drifts using closely spaced low-cost scintillation monitors (ScintPi) and multi-constellation GNSS signals

**J. Gomez Socola***,[1], F. S. Rodrigues[1], I. Paulino[2], and R. Buriti[2]

1. The University of Texas at Dallas, USA | 2. Federal University of Campina Grande, Brazil

ScintPi
Enabling Research and Education

## ABSTRACT

Previously (CEDAR 2023), we presented results of low-latitude ionospheric irregularity zonal drift measurements using closely spaced low-cost scintillation monitors (ScintPi) and signals from a geostationary satellite. The use of signals from a geostationary satellite greatly simplifies the estimation of the drifts since ionospheric pierce point (IPP) velocity and geomagnetic field varying configurations with respect to the geomagnetic field do not have to be considered. ScintPi, however, can measure signals from **multiple GNSS constellations**. The use of GNSS signals allows a broader coverage of the sky than GPS-only receivers, which have been used in previous works. In this poster, we present and discuss results of the scintillation spaced receiver technique to estimate zonal irregularity drifts using multiple GNSS signals.

## EXPERIMENTAL SETUP

In Figure 1, we show the experimental setup located at *Universidade Federal de Campina Grande* (UFCG), Brazil (7.213°S, 35.907°W, dip latitude ~14°S). UFCG is located at ~14° dip latitude where L-Band scintillations occur frequently as a result of small-scale irregularities within plasma bubbles.

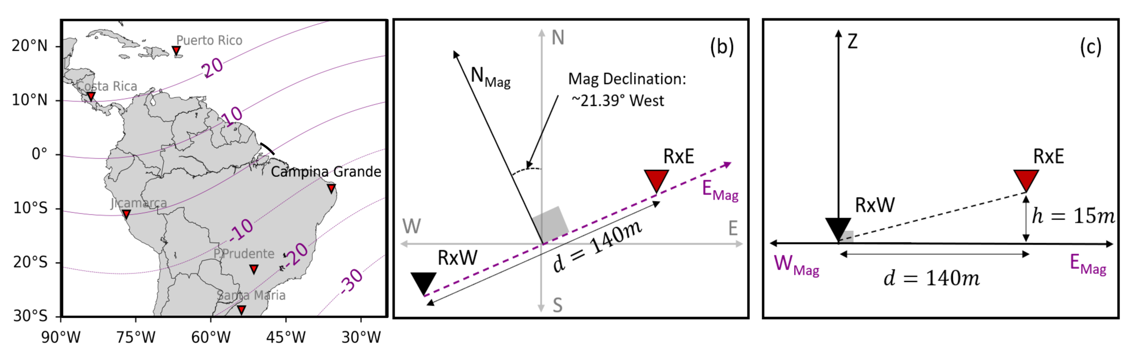


**Fig. 1** - *(a) Overview map indicating the experimental setup location and the field of view (FOV). (b) and (c) provide close-up sketches of the installation sites of the monitors along the magnetic zonal direction.*

## RELEVANCE & GOALS

This effort is well aligned with CEDAR Strategic Thrust #4: "Develop observational and instrumentation strategies for geospace system studies." We contribute with an assessment of the use of low-cost commercial off-the-shelf (COTS) GNSS receivers for observations of ionospheric irregularities. The specific goals of this work are: **(A)** to produce new ionospheric irregularity drift measurements and, **(B)** assess the response of irregularity drifts to underlying geospace conditions such us the different seasons.

## THEORY

According to Ledvina et al., (2004), the scintillation pattern propagates zonally with a velocity ($\vec{v}_{scint}$) that depends on the satellite velocity ($\vec{v}_{sat}$) and the irregularity drift ($\vec{v}_{ion}$), as described by **Equation 1**.

**[Eq. 1]**

$$v_{scintx} = \frac{z_{sat}}{(Z_{sat}-Z_{ion})}\left\{\begin{array}{c} v_{ionx} + \left(\frac{q_y}{q_x}\right) v_{iony} + \left(\frac{q_z}{q_x}\right) v_{ionz} \\ -\frac{Z_{ion}}{Z_{sat}}\left[v_{satx} + \left(\frac{q_y}{q_x}\right) v_{saty} + \left(\frac{q_z}{q_x}\right) v_{satz}\right] \end{array}\right\}$$

Where $Z_{sat}, Z_{ion}$ refer to satellite and irregularity layer scattering height, respectively. $\vec{q}$ is a vector normal to the plane containing the receiver-satellite vector ($\vec{r}_{sat}$) and the orientation of the scintillation-causing irregularities at the IPP location.

Ionospheric irregularities causing low-latitude scintillation are associated with equatorial plasma bubbles and are assumed to be aligned with the magnetic field ($\vec{B}$). See Figure 2 for an illustration of the geometry.

**Fig. 2**

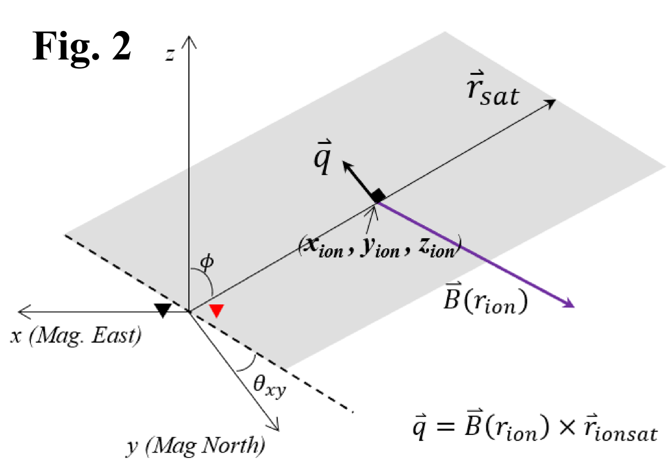


## DATA PROCESSING WORKFLOW

The estimation of scintillation pattern velocity requires one to: **(1)** calculate **satellite velocities** using information from Precise Ephemeris (SP3) files and get the **magnetic components** at the IPP from IGRF-13, **(2)** estimate the **apparent velocity** from the closely spaced scintillation monitors, **(3)** correct for any decorrelation-generated by **turbulence of the medium**, and, finally, **(4)** calculate **geometrical corrections** for any non-ideal position in the setup of the receivers (See Figure 3).

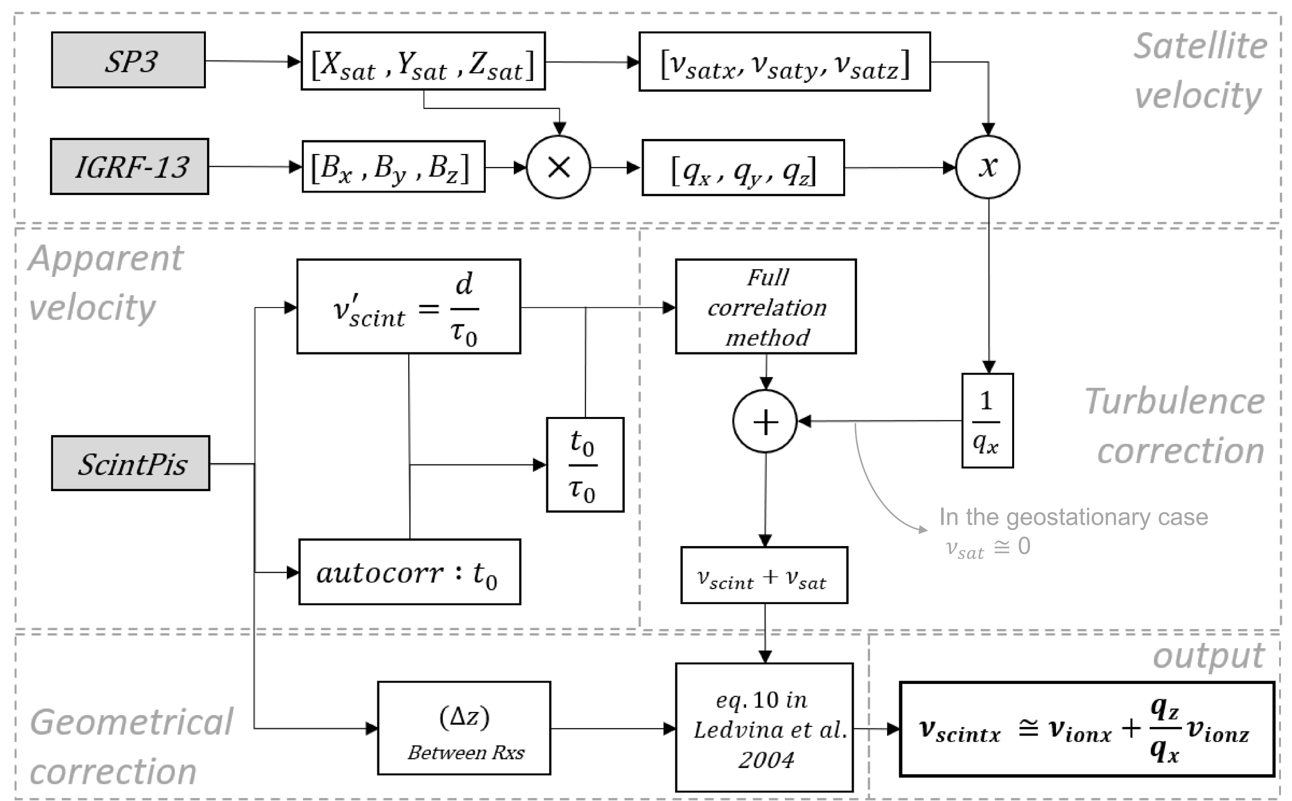


**Fig. 3** – *Workflow to estimate irregularity drifts. Inputs are represented by gray blocks. Required processes (**1,2,3** and **4**) have been divided in blocks*

## SINGLE-SATELLITE MEASUREMENTS

We now present and explain the C/No measurements made by the UFCG ScintPi monitors and how the irregularity drifts are derived from these measurements. Figure 4 shows a representative example for the Galileo 08 satellite. The measurements are for the night between Oct. 30 and 31, 2022.

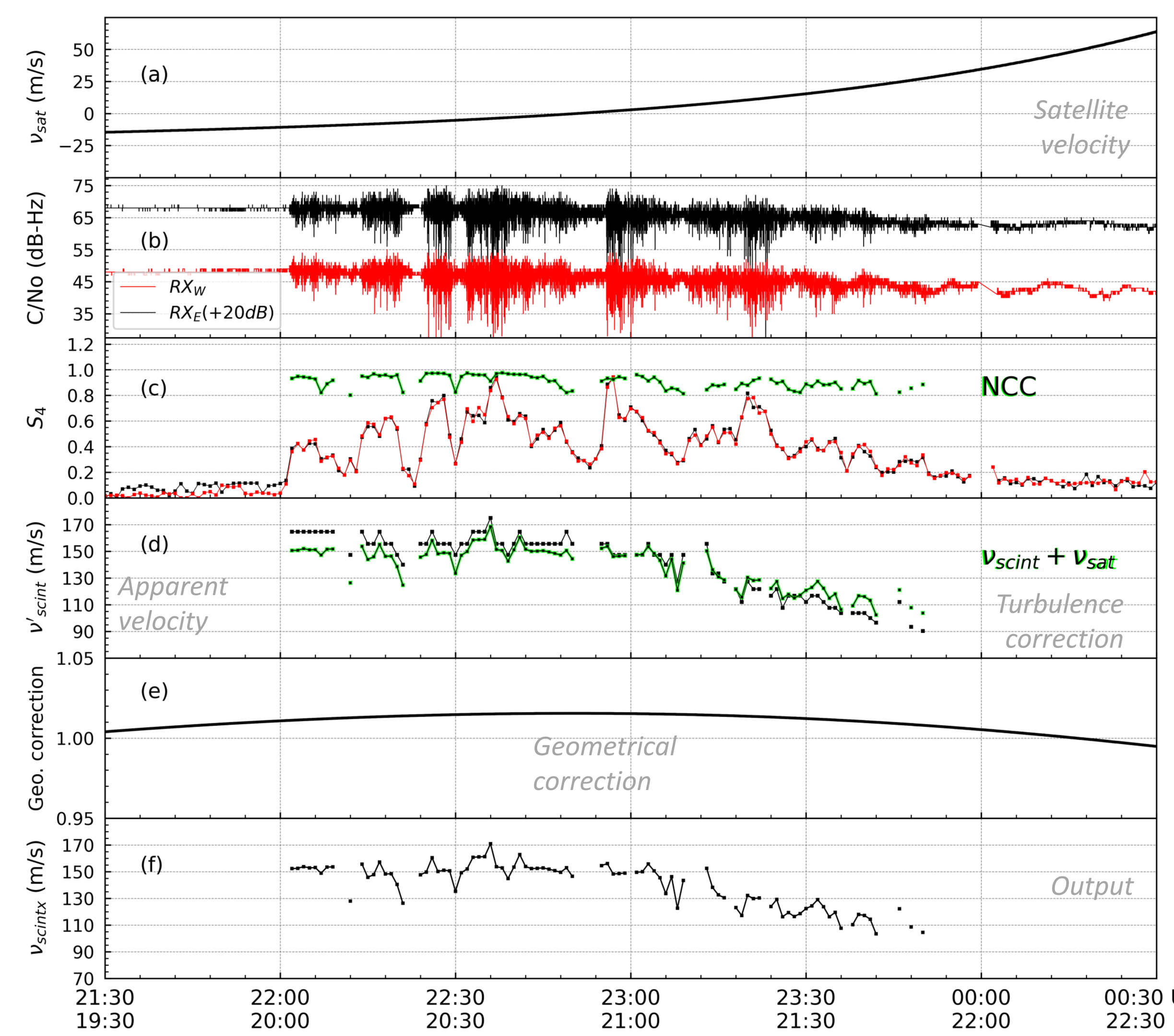


**Fig. 4** – *(a) Estimated satellite velocities from the SP3 files (b) Carrier-to-Noise ratios (C/No) in dB-Hz from $L_1$ (c) Severity of scintillation, i.e., $S_4$ index and the normalized cross correlation coefficient (NNC) (d) Apparent velocity and True satellite compensated velocity after turbulence correction (e) Geometric correction factor (f) Geometrically corrected true scintillation pattern velocity ($v_{scintx}$) representing zonal and vertical irregularity drifts.*

Eq. 1 shows that $v_{scintx}$ has contribution from two components: the zonal drift and the vertical ionospheric drift. The meridional drift ($v_{iony}$) does not have to be considered since irregularities are assumed to be elongated along the magnetic field lines.

## MULTI-SATELLITE MEASUREMENTS

The analysis illustrated in **Figure 4** is performed for any satellite that experience scintillation. For instance, all the GNSS satellites for each constellation in the night of March 22-23, 2023, are shown as an example of the process (**Figure 5a-e**). The average velocity is shown in **Figure 5f.**

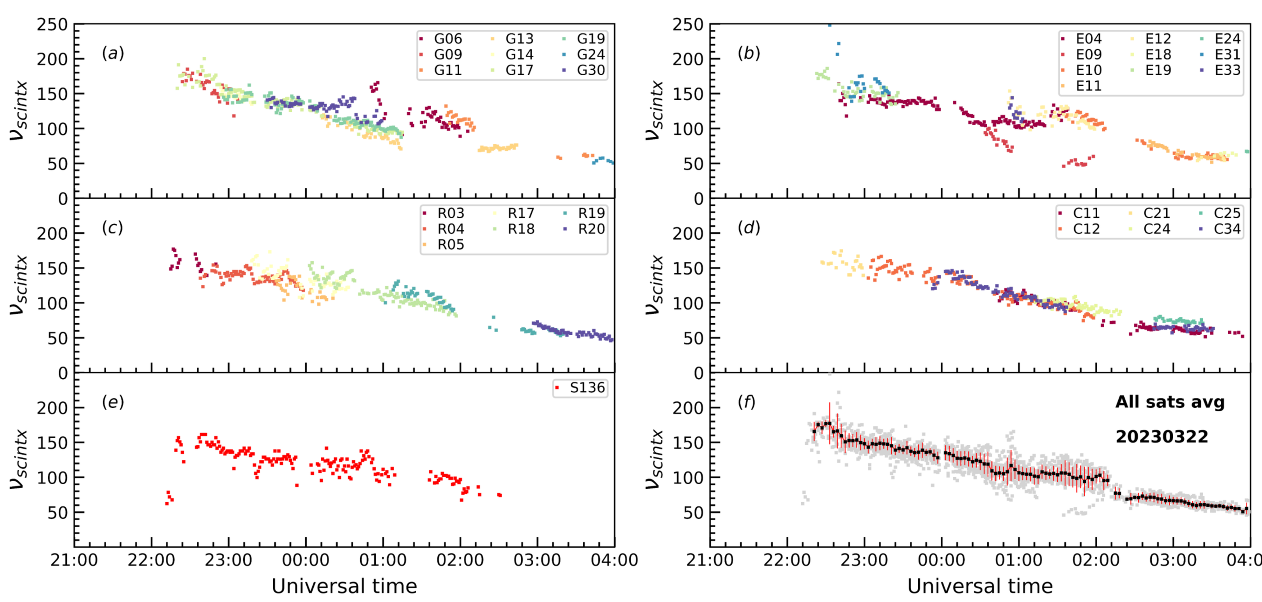


**Fig. 5** – *Scintillation pattern velocities for a full night from March 22 to 23, 2023. Measurements are separated by constellations (a) **GPS**, (b) **Galileo**, (c) **GLONASS**, (d) **Beidou** and (e) **SBAS**. Black dots in panel (f) correspond to 3-min **averaged measurements** whenever at least two satellites were available. The red bars represent 1 standard deviation.*

The goal of using multiple constellations is to gain temporal and spatial coverage. In the literature, at least a couple of approaches are used to derive irregularity drift curves. One approach averages all the measurements within the same time interval, minimizing the factor $(q_z/q_x)$ that controls the contribution of the vertical drifts in **Equation 1** (Ledvina et al., 2004). Another approach is to use only measurements where $q_z/q_x$ is small (say, less than 0.05), which also minimizes the contribution from the vertical component of the drifts (Cerruti et al., 2006). Here, we take the first approach, averaging all the drifts in 3-minute time windows, as done in **Figure 5f**.

**Figure 5f** also shows the existence of moderate variance in the irregularity drifts. The variability is more pronounced at the beginning of the night. These variations can represent either the random behavior of the horizontal and vertical plasma motion or different longitudinal contributions of vertical drifts within the field of view.

## CLIMATOLOGY

The irregularity drifts were estimated for each day during the 2022-2023 Equatorial Spread-F (ESF) season, from September 2022 to April 2023. Our results (**Figure 6a**) show the day-to-day variability of the drifts but also a seasonal trend which may be driven, primarily, by neutral winds.

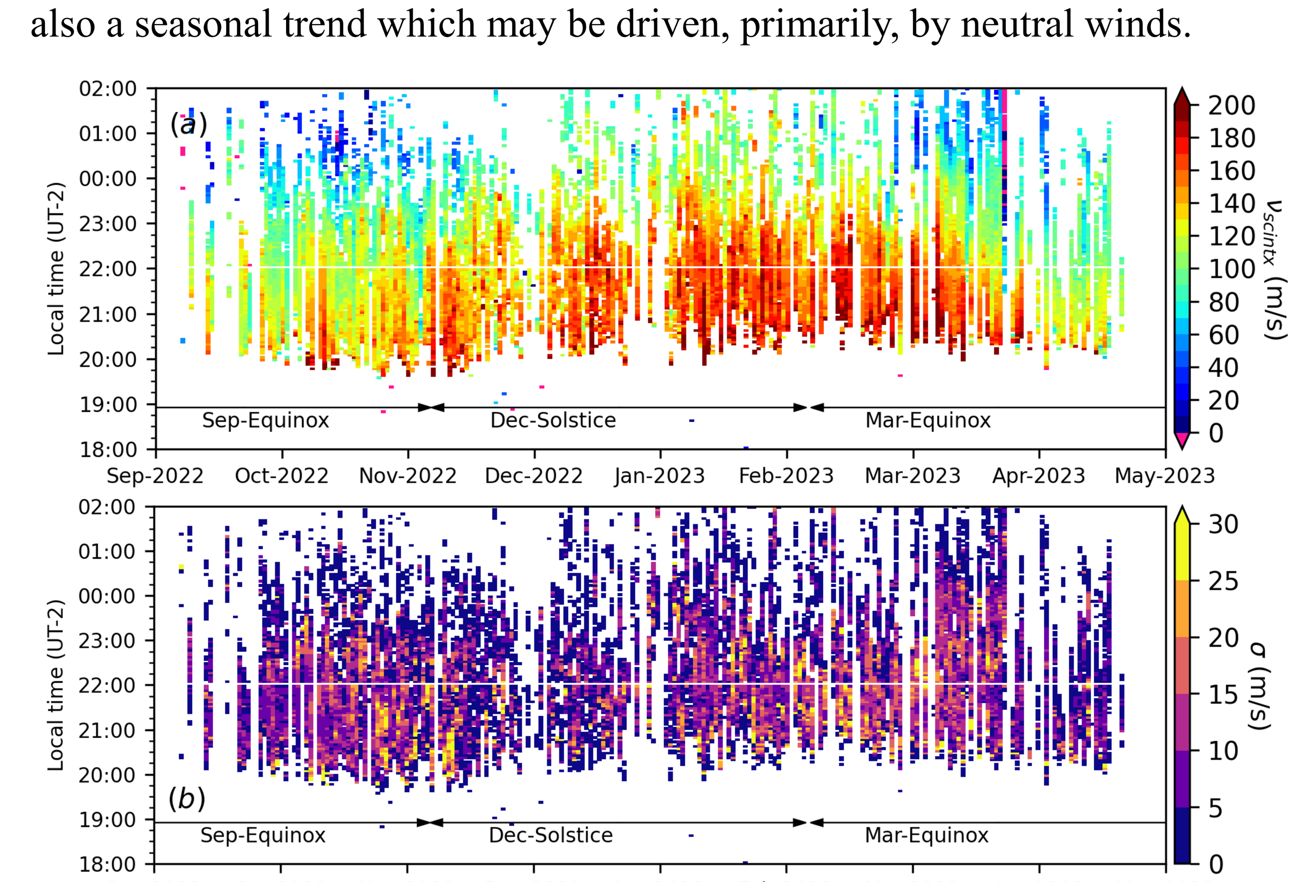


**Fig. 6** – *Panel (a) shows 3-min averaged irregularity drift. (b) Standard deviations for each 3-min average drift. Different seasons determined as +/- 45 days around equinox and solstice days are also indicated.*

## VALIDATION BY CROSS-OBSERVATIONS

While the standard deviation of the averaged drifts exceeds 25 m/s at times (**Figure 6b**), the difference between independent measurements within the same angle of arrival (i.e., within 3° elevation and within 6° azimuthal angle) are less than 20 m/s for 90% of the observations. See **Figure 7** below.

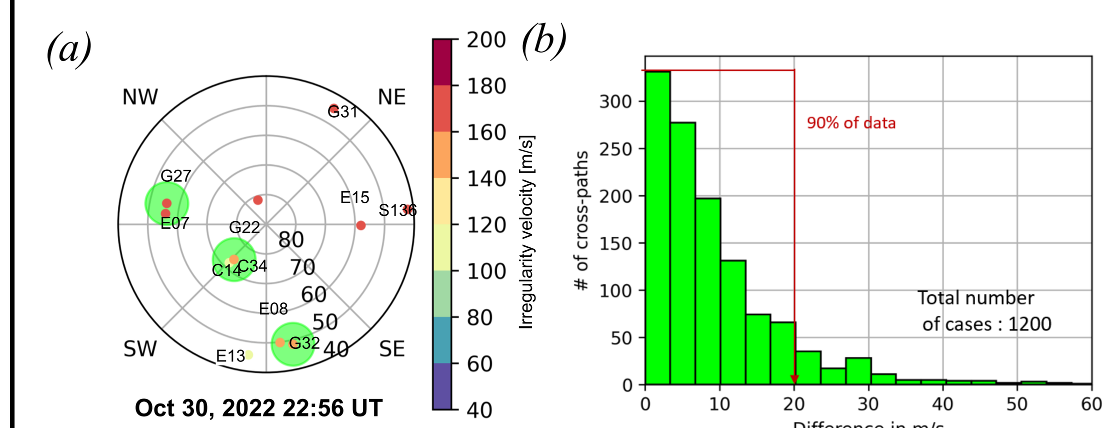


**Fig. 7** – (a) *Highlighted in green are examples of measurements within the same angle of arrival. Panel (b) statistics for the differences between the crossed observations. Around 1,200 crossing were detected during the campaign.*

The small difference between the measurements indicates that our velocities agree very well between independent measurements, which means that the spaced-receiver technique captures geophysical drifts variations in any sub-region within the field of view. Differences greater than 20 m/s represent only ~10% of the cross-paths, and those errors can be caused by the accentuated quantization effects (low C/No resolution of ScintPi monitors) for high drift values or by strong turbulence in the region of observations.

## CONCLUDING REMARKS

- In this study, we presented new measurements of low-latitude ionospheric irregularity drifts using GNSS signals (**Figures 4 and 5**) measured by alternative, low-cost scintillation monitors (**Goal A**).
- We used the scintillation spaced-receiver technique introduced by Briggs et al. (1950) and improved by Ledvina et al. (2004).
- The averaged zonal irregularity drifts show significant variance (> 25 m/s) at times (**see Figure 6b**) which can be attributed to spatial variations in the drifts within the FOV of the monitor. Even measurements from nearly the same ionospheric region but using different GNSS signals show differences (< 20 m/s for 90% of cases) in drift estimates.
- Seasonal trends can be identified in the drifts within a ESF season (**Figure 6a**) which are attributed to seasonal variations in the thermospheric neutral winds.(**Goal B**)

## ACKNOWLEDGEMENTS

This work has been supported by the National Science Foundation, Award AGS 2122639.

## REFERENCES

- Gomez Socola, J., Rodrigues, F.S. (2022), ScintPi 2.0 and 3.0: low-cost GNSS-based monitors of ionospheric scintillation and total electron content. Earth Planets Space 74, 185.
- Briggs, B. H., Phillips, G. J., & Shinn, D. H. (1950). The analysis of observations on spaced receivers of the fading of radio signals. Proceedings of the Physical Society. Section B, 63(2), 106–121. https://doi.org/10.1088/0370-1301/63/2/305
- Ledvina, B. M., Kintner, P. M., and de Paula, E. R. (2004), Understanding spaced-receiver zonal velocity estimation, J. Geophys. Res., 109, A10306, doi:10.1029/2004JA010489.
- Cerruti, A. P., B. M. Ledvina, and P. M. Kintner (2006), Scattering height estimation using scintillating Wide Area Augmentation System/Satellite Based Augmentation System and GPS satellite signals, Radio Sci., 41, RS6S26, doi:10.1029/2005RS003405.